Postprint of: Panuszko A., Nowak M., Bruździak P., Stasiulewicz M., Stangret J.: Amides as models to study the hydration of proteins and peptides —spectroscopic and theoretical approach on hydration in various temperatures. JOURNAL OF MOLECULAR LIQUIDS. Vol. 278 (2019), pp.706-715. DOI: 10.1016/j.molliq.2019.01.086

Amides as models to study the hydration of proteins and peptides - spectroscopic and theoretical approach on hydration in various temperatures

A. Panuszko[☆], M.G. Nowak, P. Bruździak, M. Stasiulewicz, and J. Stangret

Department of Physical Chemistry, Chemical Faculty, Gdańsk University of Technology, Narutowicza 11/12, 80-233 Gdańsk, Poland

Abstract

Interactions with water are one of the key factors which determine protein stability and activity in aqueous solutions. However, the protein hydration is still insufficiently understood. *N*-methylacetamide (NMA) is regarded as a minimal part of the peptide backbone and the relative simplicity of its structure makes it a good model for studies on protein–water interactions.

In this paper, the influence of NMA and *N,N*-dimethylacetamide (DMA) on surrounding water molecules in a range of temperature (25–75 °C) is studied by means of the FTIR spectroscopy. The results of the difference HDO spectra method are compared with the results of theoretical DFT calculations of NMA and DMA aqueous complexes.

Both NMA and DMA can be regarded as "structure-makers", yet their hydration spheres are different. These molecules exhibit a mixed and mutually dependent types of hydration: hydrophilic and hydrophobic. In the case of a NMA molecule that has one methyl group less than DMA, the type of

[☆]Corresponding author: *aneta.panuszko@pg.edu.pl*

hydrophobic hydration is more important. The DMA hydration sphere is less stable: the interactions between water molecules around the methyl groups are strained. Moreover, the hydration of NMA is much more temperature dependant than in the case of DMA. The source of the differences may be hidden in the N–H$\cdots$H$_2$O interaction.

The delicate nature of water interactions with the peptide block models may be cautiously translated into the much more complicated interactions of proteins with their hydration shells.

Keywords: *N*-methylacetamide, hydration, FT-IR spectroscopy, DFT calculations

1. Introduction

Proteins play key role in every biological process. Their functionality in living organism is determined by their secondary and tertiary structure, which is formed and preserved by relatively weak interactions called hydrogen bonds. Hydrogen bonds in protein-water systems consist mostly of intra- and intermolecular bonds between protein molecule and water in natural environment.

Interactions of water and proteins is one of the most important topics when it comes to studying behavior of proteins in their native state. Multiple studies have taken on this topic using various methods [1–12], however, it is still poorly understood. The study of proteins hydration experimentally is problematic due to the high level of complexity of these molecules. Additionally, overall hydration of proteins involves two general types of interactions, namely, hydrophilic hydration and hydrophobic hydration of the non-polar

fragments. Those contributions are hard to separate in such complex structures.

N-methylacetamide (NMA) can be regarded as a single peptide bond unit that is used as a model for studying both intra- and intermolecular interactions that would occur within proteins backbone in their native states. It has been shown that the NMA's hydration sphere is very similar to the hydration sphere of lysozyme. The lysozyme-affected water spectrum mainly consists of the spectral share of water affected by NMA, which indicates the hydration of the protein backbone.[12] Recent studies have confirmed the resemblance of NMA to peptides as it seemed to form chain like structures similar to protein backbone [13]. Existence of NMA dimers and other oligomers have also been proposed [14–17]. Particularly, it was pointed out that NMA dimer might be even more convenient peptide bond model than NMA itself [15].

NMA and its water clusters have been extensively studied both experimentally [13–15, 18–28] (mainly by means of vibrational spectroscopy) and theoretically [13, 15, 18, 19, 25, 27–35]. It has been numerously investigated using C=O or N–D stretch as a probe of changes in its surrounding [13, 14, 18, 19, 26, 28–30]. Changes of water OD bands in isotopically diluted systems is also a popular probe for studying hydration of NMA [18, 34, 36]. Using aforementioned approach it has been stated that at 25^{o}C water in NMAs first hydration shell forms stronger hydrogen bonds than bulk water [36]. Recently, these observations have been supported by Salamatova *et. al* [18], with the results of MD simulations of NMA–water systems. Theoretical studies describing this molecule's hydration have shown that a water molecule forms stronger hydrogen bonds with the C=O group than with the N–H or

N–D [29, 37–39]. Also, it has been observed that C=O$\cdots$$H_2O$ hydrogen bonds are stronger than between water molecules. However, computational studies of deuterated systems carried out by Yadav *et al.* [29] revealed that bonds formed by the C=O group and water are weaker than water–water hydrogen bonds outside NMA first hydration shell.

In other works, in which the hydration of this molecule was investigated, it has been pointed out that the dilution of the bulk NMA with water or the increase of temperature leads to the disruption of hydrogen bonded aggregates present in the bulk NMA at low temperatures [33]. Its hydration leads to the formation of NMA–water clusters in which at least some of NMA dynamics seems to "freeze at a measurable time scale. This means that NMA experiences a kind of hydrophobic collapse while interacting with water [18]. The *ab initio* analysis of 1·NMA–2·H_2O clusters and their deuterated derivatives has allowed to assign normal modes of the aqueous hydrogen bonded NMA [34]. The one water molecule has been hydrogen bonded to C=O group of NMA and another one to the N–H group of those molecule.

Yang and Qian [40] conducted MM studies on properties of the isolated *cis*- and *trans*-NMA and NMA–water complexes. Calculation of the interaction energies and cooperative effect have revealed that complex of the *trans*-NMA with two water molecules attached to the carbonyl oxygen is energetically unfavorable. Buck and Karplus on the basis of MD in a vacuum [39] have found that in the case of such a complex distance between the hydrogen atom of the first water molecule and the carbonyl oxygen atom is 1.71 Å and the second is 1.97 Å. Also, it has been shown that NMA with one hydrogen bonded water molecule on either C=O or N–H prefers a second one interact-

ing with the other group [40]. In addition, it has been found that complex with 3 water molecules is stable.

Several studies focus on a *cis–trans* equilibrium caused by rotation barrier around C–N bond in formamide and acetamide derivatives [23, 41–45]. It has been shown that in the case of NMA similarly to proteins *trans* form of NMA is the dominant form in liquid phases. This form also dominates in the gas phase. Theoretical studies on properties of isolated NMA molecule and NMA in aqueous solution revealed also the existence of two other resonance structures in such systems [38, 46–48]. Neutral form of NMA is more pronounced in gas phase while zwitterionic structure in water. As a result, the elongation of C=O bond and the shortening of N–C bond passing from gas to water are observed. This effect is caused by the stabilization of zwitterionic structure of NMA by hydrogen bonding with water molecules. Also, the rotation of the amide methyl group as an effect of solvation NMA molecule has been observed.

The Born–Oppenheimer molecular dynamics and MD/MM have been used to study NMA in the gas phase and in a box of water molecules [48]. The resultant frequencies of the amide bond vibrations confirmed other theoretical and experimental studies [49, 50].

In this work we have investigated the water structure around NMA in wide temperature range by means of the FTIR spectroscopy. Vibrational spectroscopy is an excellent method for investigation of solute hydration [51, 52]. Isotopic dilution technique of HDO in water allows us to obtain bands which are more convenient to analyze and highly sensitive to changes in a solution. HDO spectra are narrower and less complex than the OH bands

of H_2O. Moreover, the OD vibration is practically free from intramolecular and intermolecular couplings between oscillators. Using difference spectra method [53–55] it is possible to isolate the contribution of HDO affected by the solute from the OD band. Solute-affected HDO spectra can then be compared with HDO spectra of bulk water, thus determining the structural and energetic state of hydrogen bonds of water in the nearest surroundings of solute. In isotopically diluted solutions of NMA there is significant amount of N-deuterated NMA. N–D bond vibrations happen to manifest in the IR spectrum in the same region as HDO bands. Spectra of water affected by *N,N*-dimethylacetamide (DMA) have also been obtained to isolate ND stretching vibration from NMA-affected HDO spectra and to compare those compounds in terms of hydration. To confirm the interpretation of spectral results theoretical calculations were performed.

2. Materials and Methods

2.1. Chemicals and Solutions

N-methylacetamide (99+%, Aldrich), *N,N*-dimethylacetamide (Acros Organics, 99.5%) and deuterium oxide (Aldrich, 99.96%) were used to prepare solutions without purification. Water used was deionized. For each solute (NMA, DMA) stock solution in deionized water of maximum molality 1 $\mathrm{mol} \cdot \mathrm{kg}^{-1}$ was prepared. Less concentrated solutions were prepared by dilution of weighed amounts of stock solutions using deionized water. Each of the solutions was then divided into two parts in order to prepare sample and reference solutions. Sample solution was prepared by adding D_2O to one of the parts in amount of 4% with respect to H_2O (by weight). Reference

solution was prepared by adding the same molar amounts of H_2O to the second part. The amount of used deuterium oxide was confirmed to be enough for reaction $H_2O + D_2O = 2HDO$ ($K \approx 4$) to give an almost quantitative amount of HDO. All solutions were prepared by weight. The prepared solutions were degassed before density and spectral measurements. Solution densities were measured using the Anton Paar DMA 5000 densitometer at all studied temperatures (25, 35, 45, 55, 65, and 75 ^{o}C, with the tolerance of 0.001 ^{o}C).

2.2. FTIR Measurements

FTIR spectra of prepared solutions were recorded on Thermo Electron Co. Nicolet 8700 spectrometer with resolution of 4 cm^{-1}. Each spectrum was an average of 128 independent scans. A liquid cell (model A145, Bruker Optics) with CaF_2 windows separated PTFE spacers was used. The path length was determined interferometrically and was 29.0 μm. The temperature of measurements was kept at 25, 35, 45, 55, 65, and 75 ^{o}C with a tolerance of $\pm$0.1 ^{o}C and monitored using electronic thermometer with thermocouples placed in the sample. The temperature of 75 ^{o}C has been chosen as an upper temperature limit being the highest possible temperature due to technical capabilities of the experimental setup. In the case of DMA solutions, the maximum temperature was limited to 55 ^{o}C due to decomposition of solution components to gaseous products at higher temperatures. The spectrometer was purged with dry nitrogen to eliminate the influence of air components on recorded spectra, namely, CO_2 and water vapor.

2.3. Spectral data analysis

Procedures of recording and analyzing spectra were handled using the commercial PC software: OMNIC (Thermo Electron Co.), GRAMS/32 (Galactic Industries Corporation, Salem, NH) and RAZOR (Spectrum Square Associates, Inc., Ithaca, NY).

To obtain the desired information the difference spectra method [56] was applied. This method assumes that water in a solution can be divided into two additive contributions: the "bulk" water—identical to pure water—and "affected" water—under the influence of solute. Therefore information about solute-affected water can be isolated from solutions IR spectrum. The detailed procedure of spectral data analysis toward extraction of the solute-affected water spectra has been described in section S1 of Supplementary Data.

2.4. Interpretation of the solute-affected water spectra

To interpret given solute-affected spectra the Badger-Bauer rule is used [57]. This empirical rule states that energy of hydrogen bonds is proportional to the shift of the OD band position, thus it is a convenient method of comparing energetic state of solute-affected water with bulk water and investigate the changes of this characteristics with temperature [54, 55]. The shape of an OD bands contain information about hydrogen bond energy distribution in water. With the existence of empirical curves that link the oxygen–oxygen intermolecular distance (R_{OO}) with the OD stretching wavenumber (ν_{OD}) it is possible to transform the spectral band shapes to the oxygen–oxygen distance distribution function $P(R_{OO})$ [56, 58].

2.5. Theoretical calculations

All calculations involving optimization of NMA or DMA complexes with water molecules were performed with the Gaussian 09 v.D1 software [59] available at the Academic Computer Center in Gdansk (TASK). The analysis of resulting wavefunction files involving electron density difference calculations and the reduced density gradient (RDG) method [60] was performed with the Multiwfn software v.3.3.9. [61]. Structures of NMA or DMA complexes with water molecules were optimized similarly to the procedure presented in our previous papers [16, 62]. Final structures were optimized at the density functional theory (DFT) level with B3LYP hybrid exchange-correlation functional [63, 64] and 6-311++G(d,p) basis set [65] within the conductor-like polarizable continuum model (CPCM) of water as a solvent [66, 67]. All calculations were performed with the D3 version of Grimme's empirical dispersion correction including Becke–Johnson damping [68]. Such a selection gives a good consistency of theoretical and experimental results.

Differences in electron densities caused by NMA or DMA interactions with water molecules were calculated and visualized according to section 4.5.5 of the Multiwfn manual. Shortly, electron densities were calculated for the water complex with NMA or DMA and separately for their isolated fragments: NMA or DMA, and water molecules, and then appropriately subtracted from each other.

3. RESULTS AND DISCUSSION

3.1. FTIR investigation of water structure

3.1.1. Characteristic of solute-affected water spectra and "bulk" water spectra

Figure 1 presents the NMA-affected HDO spectra (Figure 1a), DMA-affected HDO spectra (Figure 1b), and the "bulk" water spectra (Figure 1c) as a function of temperature. Band shapes of these spectra were transformed into the oxygen–oxygen distance distribution function $P(R_{OO})$ of the water molecules. The obtained distance probability distributions are shown in Figs. 2a and 2b for solute-affected water, $P^a(R_{OO})$, and in Figure 2c for "bulk" water, $P^b(R_{OO})$. The band parameters for affected HDO bands, together with the bulk HDO bands, for measured temperatures are presented in Table 1, along with intermolecular oxygen-oxygen distances, R_{OO}.

A comparison of the values of the mean oxygen–oxygen distances (R^g_{OO}) for solute-affected water and for "bulk" water (Table 1) points out that water-water hydrogen bonds are shorter in the presence of these solutes. The shift of the values of the gravity center of bands, ν^g_{OD}, (related to the mean energy of water hydrogen bonds) towards lower values with respect to the ones corresponding to pure water at a given temperature (Table 1) suggests that water affected by NMA and DMA forms on average stronger H-bonds than pure water in the whole temperature range. In addition, the hydrogen bonds of water molecules around NMA are stronger and shorter than those in water affected by DMA. The above results indicate that both amides enhance the water structure in their nearest surrounding in the whole temperature range, and can be classified as "structure-making" solutes. This statement is supported by the analysis of radial distribution functions obtained by means

of MD simulations at 27^{o}C [18]. Analyzing the effect of temperature variation on the affected HDO spectra, it can be seen that solute-affected water spectra at lower temperature are characterized by stronger hydrogen bonds than at higher temperatures. A similar relationship is shown by the "bulk" water spectrum. This is obvious because at higher temperatures the distances between water molecules increase and hydrogen bonds weaken. Furthermore, the number of moles of affected water molecules (N values from Table 1) around NMA decreases as the temperature increases, and as a result at the highest temperature, the two water molecules are affected by NMA. Water molecules in the hydration sphere of DMA are not susceptible to temperature variations, which is reflected the constant value of number of affected water molecules as a function of temperature.

3.1.2. Differences in oxygen-oxygen distance distributions between "affected water" and "bulk" water

To provide greater insight into the difference in intermolecular distances between affected water and "bulk" water the following procedure was used: the distance distribution function for "bulk" water, $P^b(R_{OO})$, (Figure 2c) was subtracted from the distribution function of water affected by solute, $P^a(R_{OO})$, (Figures 2a and 2b) at a given temperature. The results of the subtraction, $\Delta P(R_{OO})$, each analyzed temperature are shown in Figures 3a and 3b for NMA and DMA, respectively. This operation allows to observe subtle changes in the population of hydrogen bonds of water affected by solute relative to "bulk" water at a given temperature.

The analysis of distance differences (Figure 3b) clearly shows that the hydration sphere of DMA contains two populations of hydrogen bonds of

water for all studied temperatures: the first one corresponds to the weak hydrogen bonds ($R_{OO} \approx 2.9$ Å), while the second one corresponds to the strong water-water hydrogen bonds ($R_{OO} \approx 2.73$ Å). The distances assigned to the second population is close to the distance typical to the water in the ice phase ($R_{OO} = 2.76$ Å) [69]. The creation of the above-mentioned populations takes place mainly at the expense of very weak hydrogen bonds ($R_{OO} \geq 3.0$ Å) and to a lesser extent of hydrogen bonds with mean energy (the population of water-water hydrogen bonds only slightly longer than and equal to the most probable distance in bulk water, value $R_{OO} = 2.826$ Å at 25 ^{o}C, see Table 1). A slightly larger population of strong water hydrogen bonds relative to the weak ones causes that in the surrounding of DMA the water structure is strengthened with respect to the "bulk" water. Furthermore, it can be seen that the differences between DMA-affected water and "bulk" water are practically the same at all temperatures. This means that DMA enhances to the same extent the water structure in the whole temperature range, and thus demonstrates the high stability of the DMA hydration shell.

A common feature of the differences in intermolecular distances distribution for NMA, $\Delta P(R_{OO})$, (Fig. 3a) is the reduction of population of very weak hydrogen bonds of water ($R_{OO} \geq 3.0$ Å) and simultaneous distinct increase the strong ones ($R_{OO} \approx 2.73$ Å), in comparison to "bulk" water. The first population is practically unchanged with increasing temperature. The most significant changes relate to the population of water molecules with mean energy and weak hydrogen bonds of water ($R_{OO} \approx 2.9$ Å). At the lowest temperatures (25 ^{o}C and 35 ^{o}C), it may be seen that population of such hydrogen bonds of water around NMA decreases, relative to the "bulk" water.

However, starting from the temperature of 45 ^{o}C, the discussed population of hydrogen bonds increases with the temperature increase.

3.1.3. Differences between $\Delta P(R_{OO})$ vs. temperature 25^{o}C

Changes in populations of hydrogen bonds in the hydration sphere of NMA, with respect to the temperature of 25 ^{o}C as a reference point, are shown in Figure 4. As can be seen, the population of water molecules with mean and weak energy of hydrogen bonds is increased in comparison to $\Delta P(R_{OO})$ at 25 ^{o}C. This population seems to be responsible for the weakening of the hydrogen bond network around NMA when the temperature increases, relative to the course of $\Delta P(R_{OO})$ at 25 ^{o}C. The NMA hydration sphere at 35 ^{o}C is additionally characterized by a slightly larger population of strong hydrogen bonds (ca. 2.65 Å) relative to the temperature of 25 ^{o}C. Probably, such a population can be caused by the formation of NMA–NMA dimers [14–16] at this temperature, which may break up at higher temperatures. Such an interpretation is however speculative because the presence of dimers in aqueous solutions is difficult to observe.

3.2. DFT calculations: sources of differences in NMA and DMA hydration

A series of DFT calculations was performed to try to explain the differences in strong and weak populations of hydrogen bonds recognized on the basis of NMA- ad DMA-affected water spectra. Undoubtedly, the difference between NMA and DMA hydration lies in the presence of additional methyl group. Thus, we created a closed ring of water molecules encircling those compounds in the closest proximity of the amine proton or methyl group in the case of NMA and DMA, respectively, by a gradual addition of water

molecules to optimized NMA and DMA structures (see Figure 5). The water ring is a model of the full hydration shell, which could be too demanding to calculate for the selected set of method and basis set. In each case, the minimal number of water molecules needed to create a closed circle of water molecules was equal to eight. Animations showing optimized structures of these complexes (in two variants: with overlaid differences in electron density or with visualized places of weak interactions determined by RDG method) are included in Supplementary data.

3.2.1. Steric effect

For both NMA and DMA the ring of water molecules is skewed (Figure 5, top view). The skewness seems to be connected with the steric effect that nitrogen-bounded methyl group exerts on water molecules approaching the carbonyl oxygen atom. The starting dihedral angle between C–H and C=O bonds in NMA or DMA isolated molecules is close to 0^o. This result is in accordance with ref. [37]. The situation changes when interactions with water molecules occur. When water molecules approach the carbonyl bond of NMA the C–H bond easily adopts the dihedral angle to ca. 30^o to fit the water ring encompassing the molecule (Figure 5, front view), hence the skewness of the water ring plane. The rotation of the amide metyl group of NMA, when going from gas phase to solution, has also been found by Mennuci *et.al* [37]. However, the examined clusters have been smaller (they contained up to 3 water molecules) and the value of the dihedral angle was different. The weak steric interaction between carbonyl group and methyl proton (marked with red arrow in Figure 6a) also shifts to one side and makes place for a water molecule to take the optimal location. The position of methyl proton

is not as fixed as in the case of DMA, where an additional steric interaction is placed between both amine methyl groups (large green/red patch under carbonyl group in Figure 6a). Moreover, carbonyl group (C=O) and water molecules interacting with it lies in one plane and the water ring is highly symmetrical (Figure 5, front view).

Interactions between water molecules or between water molecules and the carbonyl group of NMA or DMA are enhanced with respect to the "bulk" structure ($R_{OO,bulk,av.} = 2.817$ Å, see Fig. S5 in Supplementary Data), thus, an enhanced population is expected to be present in the R_{OO} distance distribution. In fact, both compounds exhibit such an enhancement (Figure 3). The population origins not only in water–carbonyl interactions but can be the effect of the hydrophobic hydration, in which van der Waals interactions have a dominant role (green/olive patches around methyl groups in Fig. 6a). In the case of formamide, i.e. a molecule that does not contain hydrophobic groups in its structure, we observe only an increasing population of weak hydrogen bonds of water, in comparison to the "bulk" water (see Fig. 8a in ref. [36]) This indicates that in the presence of formamide, the hydrogen bonds between water molecules and the oxygen atom of carbonyl group and those between water molecules are weaker.

The interaction of carbonyl group of NMA with a single water molecule does not seem to be distinguished, and its energetics is similar to the one between water molecules [16, 29]. However, the closing of the water ring around NMA, involving weak hydrophobic interactions (green/olive patches in Fig. 6a), enhances significantly C=O$\cdots$H$_2$O binding. In such a situation, two water molecules interact strongly with carbonyl oxygen and almost to

the same degree (R_{OO} = 2.710 Å and 2.728 Å). Similar length (2.73 Å) beetween carbonyl oxygen and water oxygen has been obtained by means of MD simulations for a larger system in ref. [38]. The shape of the electron density differences caused by the interaction of NMA and the water ring confirms high similarity, or symmetry, in both water–carbonyl interactions.

Further analysis shows that under the influence of water molecules the electron density increases on the carbonyl oxygen. This is accompanied with the decrease of electron density along the C=O bond. Also, the decrease of electron on the amide hydrogen and its increase along the N–H bond towards the nitrogen atom can be observed. In addition, electrons of N–C bond are pushed towards the carbon atom. This results are in agreement with the analysis of Wannier Centers average positions for NMA molecule in gas phase and in water given in ref. [38]

A different picture emerges from the analysis of an analogous DMA data. Such a water ring closure in the DMA system is less favorable. The van der Waals interactions are less organized and differences in C=O$\cdots$H$_2$O interactions are larger than in the case of NMA. The introduction of additional methyl group simply inhibits the rotation of other two methyl groups in DMA molecule. The nitrogen-bonded methyl group of DMA cannot adopt an optimal angle to fit the water ring as in NMA system. This way, only one water molecule of water can easily interact with the carbonyl group while the second one has to find another—non-optimal with respect to NMA—place at the expense of the interaction energy with the carbonyl group. One water molecule is closer to the carbonyl oxygen atom (R_{OO} = 2.705 Å), while the second one interacts poorly (R_{OO} = 2.886 Å, higher even than the average

"bulk" distance). Such an inequality may contribute to the presence of two distinct water hydrogen bond populations (stronger and weaker relative to the "bulk" water) in the vicinity of DMA molecule, as in experimental results presented in Figure 3. It should be stressed that the population of strong hydrogen bonds includes also interactions between water molecules around methyl groups. The symmetry of water–carbonyl bond–water double interaction is broken. Such a division is also clearly visible in the electron density difference (Figure 5, top view), where the weakly interacting water molecule is pushed away from the plane of the water ring. The change in electron density for the first water molecule is highly similar to the case of NMA, while the second one is non-symmetrical and exhibits a weaker electron density transfer.

According to the above discussion, the differences in the hydration properties of both molecules are related to the formation of a water cage around them. Both NMA and DMA due to the presence of hydrophilic and hydrophobic groups in their molecule are characterized by two types of hydration, which are mutually dependent. Moreover, hydrogen bonds between water molecules involved in the cage formation and the interaction of water molecules with the carbonyl oxygen atom are cooperative. The formation of a water cage around hydrophobic groups affects the equality/inequality of interactions of water molecules with the carbonyl group. In the NMA molecule, the hydrophobic type of hydration is more important, although it has one methyl group less than DMA. This is due to a worse fit of the "ice-like" water around methyl groups of DMA to the molecular shape of the molecule.

3.2.2. Importance of N–H$\cdots H_2O$ interaction

The interaction of water molecule with hydrogen atom of amino group of NMA ensures the stability of the hydration sphere around NMA. It acts like a "clip" stabilizing the hydration cage around NMA. At lower temperatures, this interaction is incorporated in the hydration cage [36]. When the temperature increases, the hydrogen bonds around NMA weaken and eventually break, and as a result, the water molecule interacting with the hydrogen atom of amino group starts to lose its contact with other water molecules. The relatively weak N–H$\cdots$water interaction (the distance between the nitrogen atom of NMA and oxygen atom of water is 2.890 Å), freed from other interactions, contributes to the increase of the population of weak hydrogen bonds in the presence of NMA at higher temperatures (see Fig.3a).

The hydration shell around DMA, represented with the modeled ring of eight water molecules, is already less stable than in the case of NMA at ambient temperatures (see Figure 6a, the van der Waals interactions are scattered much more than in the case of NMA). The ring of water molecules around DMA is stretched from the very beginning due to the relatively large methyl group in the place of amine proton. In consequence, the already weakened hydration shell may be less prone to the temperature increase.

4. Conclusions

The effect of NMA and DMA on the water structure as a function of temperature has been studied by means of FTIR spectroscopy, supported with DFT calculations. The results of theoretical calculations helped to resolve spectral results. The agreement between experimental and computational re-

sults was satisfactory and gave a consistent picture of the amides hydration in aqueous solution.

The results revealed that hydrogen bonds of water molecules around these solutes are stronger and shorter than those in pure water in the whole temperature range. Although both solutes strengthened the water structure, significant differences in the characteristics of their hydration shells could be noticed. The essential difference in the hydration of NMA and DMA is the way they create the water cage around them, which is the result of both hydrophilic and hydrophobic hydration. These two types of hydration are mutually dependent. Thus, the increase in the population of strong hydrogen bonds of water in the surroundings of these solutes is the effect of the interactions of water molecules with the oxygen atom of carbonyl group and those between water molecules around hydrophobic groups. The hydration sphere of formamide, a molecule that does not contain any hydrophobic group, is characterized by an increased population of weak hydrogen bonds of water, with respect to the "bulk" water ref. [36], without the strengthening observed in the case of NMA or DMA. This suggest that the presence of a hydrophobic element in the molecule is a factor conditioning the enhanced network of hydrogen bonds around the solute.

The DMA molecule is additionally surrounded by a population of water molecules that forms weak hydrogen bonds with respect to the "bulk" water (at all given temperatures). The presence of this population results from the poor fit of the water cage to the solute's geometry. Such a disadvantageous fit turn out to be less susceptible to the temperature change because the hydration cage is already distorted at lower temperatures, in comparison to

NMA.

On the other hand, the NMA water cage is better organized than in the case of DMA. The hydrophobic type of hydration is more important in the case of NMA molecule, although it has one methyl group less than DMA. The interaction of water molecule with the hydrogen atom of amino group is significant for the stability of the hydration sphere of NMA. Thus, at lower temperatures the hydration sphere of NMA contains only the population of stronger hydrogen bonds, in comparison to the "bulk" water. As the temperature increases, the additional population of water molecules, characterized with weak hydrogen bonds, is observed in the water population affected by NMA. It results from the weak N–H$\cdots$water interaction. At lower temperatures, this interaction is incorporated into the hydration cage, while at higher temperatures it starts to be exposed when water molecule interacting with the hydrogen atom of amino group loses its contact with the cage around the molecule.

Although both NMA and DMA are simple molecules, their similarity to the basic building block of proteins makes them convenient models of protein–water interactions. The obtained results clearly show that the contributions to the hydration sphere of the solute are not additive due to the number of non-polar groups. A stable hydration sphere depends on the possibility of building a cooperatively reinforced network of hydrogen bonding water molecules around the solutes. The changes in the hydration of solutes caused by the temperature increase and their explanation may be cautiously translated into phenomena accompanying the process of protein denaturation.

5. Acknowledgements

This work was funded by the National Science Centre, Poland (grant 2017/26/D/NZ1/00497). Calculations were carried out at the Academic Computer Centre in Gdańsk.

6. Declaration of interest

The authors declare that they have no conflict of interest.

7. References

[1] L. Biedermannova, B. Schneider, Hydration of proteins and nucleic acids: Advances in experiment and theory. A review, Biochim. Biophys. Acta 1860 (2016) 1821–1835.

[2] L. Aggarwal, P. Biswas, Hydration water distribution around intrinsically disordered proteins, J. Phys. Chem. B 122 (2018) 4206–4218.

[3] J. N. Dahanayake, K. R. Mitchell-Koch, Entropy connects water structure and dynamics in protein hydration layers, Phys. Chem. Chem. Phys. 20 (2018) 14765–14777.

[4] J. T. King, K. J. Kubarych, Site-specific coupling of hydration water and protein flexibility studied in solution with ultrafast 2D-IR spectroscopy, J. Am. Chem. Soc. 134 (2012) 18705–18712.

[5] R. C. Remsing, E. Xi, A. J. Patel, Protein hydration thermodynamics: The influence of flexibility and salt on hydrophobin II hydration, J. Phys. Chem. B. 122 (2018) 3635–3646.

[6] V. M. Dadarlat, C. B. Post, Decomposition of protein experimental compressibility into intrinsic and hydration shell contributions, Biophys. J. 91 (2006) 4544–4554.

[7] D. Hecht, L. Tadesse, L. Walters, Correlating hydration shell structure with amino acid hydrophobicity, J. Am. Chem. Soc. 115 (1993) 3336–3337.

[8] V. P. Kutyshenko, A study of water-protein interactions by high-resolution NMR spectroscopy, Mol. Biol. 35 (2001) 90–99.

[9] D. Russo, J. Olivier, J. Teixeira, Water hydrogen bond analysis on hydrophilic and hydrophobic biomolecule sites, Phys. Chem. Chem. Phys. 10 (2008) 4968–4974.

[10] M. Tarek, D. J. Tobias, The dynamics of protein hydration water: A quantitative comparison of Molecular Dynamics simulations and neutron-scattering experiments, Biophys. J. 79 (2000) 3244–3257.

[11] G. Zaccai, The dynamics of protein hydration water: A quantitative comparison of Molecular Dynamics simulations and neutron-scattering experiments, Phil. Trans. R. Soc. Lond. B 359 (2004) 1269–1275.

[12] A. Panuszko, M. Wojciechowski, P. Bruździak, P. W. Rakowska, J. Stangret, Characteristics of hydration water around hen egg lysozyme as the protein model in aqueous solution. FTIR spectroscopy and molecular dynamics simulation, Physical Chemistry Chemical Physics 14 (2012) 15765.

[13] Y. Zhou, G. Deng, Y.-Z. Zheng, J. Xu, H. Ashraf, Z.-W. Yu, Evidences for cooperative resonance-assisted hydrogen bonds in protein secondary structure analogs, Sci. Rep. 6 (2016) 36932.

[14] M. Albrecht, C. A. Rice, M. A. Suhm, Elementary peptide motifs in the gas phase: Ftir aggregation study of formamide, acetamide, N-methylformamide, and N-methylacetamide, J. Phys. Chem. A 112 (2008) 7530–7542.

[15] T. Forsting, H. C. Gottshalk, B. Hartwig, M. Mons, M. A. Suhm, Correcting the record: the dimers and trimers of trans-N-methylacetamide, Phys. Chem. Chem. Phys 19 (2017) 10727–10737.

[16] K. A. Biernacki, E. Kaczkowska, P. Bruździak, Aqueous solutions of NMA, Na_2HPO_4, and NaH_2PO_4 as models for interaction studies in phosphate–protein systems, Journal of Molecular Liquids 265 (2018) 361–371.

[17] W. A. Herrebout, K. Clou, H. O. Desseyn, Vibrational spectroscopy of N-methylacetamide revisited, J. Phys. Chem. A 105 (2001) 4865–4881.

[18] E. Salamatova, A. V. Cunha, R. Bloem, S. J. Roeters, S. Woutersen, T. L. C. Jansen, M. S. Pshenichnikov, Hydrophobic collapse in N-methylacetamide-water mixtures, J. Phys. Chem. A 122 (2018) 2468–247.

[19] L. C. Mayne, B. Hudson, Resonance Raman spectroscopy of N-methylacetamide: Overtones and combinations of the C-N stretch

(Amide II) and effect of solvation on the C=O stretch (Amide I) intensity, J. Phys. Chem. 95 (1991) 2962–2967.

[20] J. M. Dudik, C. R. Johnson, S. A. Asher, UV resonance Raman studies of acetone, acetamide, and N-methylacetamide: Models for the peptide bond, J. Phys. Chem. 89 (1985) 3805–3814.

[21] X. G. Chen, R. Schweitzer-Stenner, N. G. Mirkin, S. A. Asher, N-methylacetamide and its hydrogen-bonded water molecules are vibrationally coupled, J. Am. Chem. Soc. 116 (1994) 11141–11142.

[22] X. G. Chen, R. Schweitzer-Stenner, S. A. Asher, N. G. Mirkin, S. Krimm, Vibrational assignments of trans-N-methylacetamide and some of its deuterated isotopomers from band decomposition of IR, visible, and resonance Raman spectra, J. Phys. Chem. 99 (1995) 3074–3083.

[23] S. Song, S. A. Asher, S. Krimm, K. D. Shaw, Ultraviolet resonance Raman studies of trans and cis peptides: Photochemical consequences of the twisted pi* excited state, J. Am. Chem. Soc. 113 (1991) 1155–1163.

[24] V. Vasylyeva, S. K. Nayak, G. Terraneo, G. Cavallo, P. Metrangolo, G. Resnati, Orthogonal halogen and hydrogen bonds involving a peptide bond model, CrystEngComm 16 (2014) 8102–8105.

[25] S. Woutersen, Y. Mu, G. Stock, P. Hamm, Hydrogen-bond lifetime measured by time-resolved 2D-IR spectroscopy: N-methylacetamide in methanol, Chemical Physics 266 (2001) 137–147.

[26] M. F. DeCamp, L. DeFlores, J. M. McCracken, A. Tokmakoff, Amide I vibrational dynamics of N-methylacetamide in polar solvents: The role of electrostatic interactions, J. Phys. Chem. B 109 (2005) 11016–11026.

[27] R. Schweitzer-Stenner, G. Sieler, Intermolecular coupling in liquid and crystalline states of trans-N-methylacetamide investigated by polarized Raman and FT-IR spectroscopies, J. Phys. Chem. A 102 (1998) 118–127.

[28] R. Zhang, H. Li, Y. Lei, S. Han, All-atom Molecular Dynamic simulations and relative NMR spectra study of weak c-h o contacts in amide-water systems, J. Phys. Chem. B 109 (2005) 7482–7487.

[29] V. K. Yadav, A. Chandra, First-principles simulation study of vibrational spectral diffusion and hydrogen bond fluctuations in aqueous solution of Nmethylacetamide, J. Phys. Chem. B 119 (2015) 9858–9867.

[30] M. H. Farag, M. F. Ruiz-Lopez, A. Bastida, G. Monard, F. Ingrosso, Hydration effect on amide I infrared bands in water: An interpretation based on an interaction energy decomposition scheme, J. Phys. Chem. B 119 (2015) 9056–9067.

[31] J. Heyda, J. C. Vincent, D. J. Tobias, J. Dzubiella, P. Jungwirth, Ion specificity at the peptide bond: Molecular Dynamics simulations of N-methylacetamide in aqueous salt solutions, J. Phys. Chem. B 114 (2010) 1213–1220.

[32] W.-G. Han, S. Suhai, Density functional studies on N-methylacetamide-water complexes, J. Phys. Chem. B 100 (1996) 3942–3949.

[33] N. T. Hunt, K. Wynne, The effect of temperature and solvation on the ultrafast dynamics of N-methylacetamide, Chem. Phys. Lett. 431 (2006) 155–159.

[34] N. G. Mirkin, S. Krimm, Ab initio vibrational analysis of isotopic derivatives of aqueous hydrogen-bonded trans-N-methylacetamide, J. Mol. Struct. 377 (1996) 219–234.

[35] J. Gao, M. Freindorf, Hybrid ab initio QM/MM simulation of N-methylacetamide in aqueous solution, J. Phys. Chem. A 101 (1997) 3182–3188.

[36] A. Panuszko, E. Gojlo, J. Zielkiewicz, M. Smiechowski, J. Krakowiak, J. Stangret, Hydration of simple amides. FTIR spectra of HDO and theoretical studies, J. Phys. Chem. B 112 (2008) 2483–2493.

[37] B. Mennucci, J. M. Martínez, How to model solvation of peptides? Insights from a quantum-mechanical and molecular dynamics study of N-methylacetamide. 1. Geometries, infrared, and ultraviolet spectra in water, Journal of Physical Chemistry B 109 (2005) 9818–9829.

[38] M. P. Gaigeot, R. Vuilleumier, M. Sprik, D. Borgis, Infrared spectroscopy of N-methylacetamide revisited by ab initio molecular dynamics simulations, Journal of Chemical Theory and Computation 1 (2005) 772–789.

[39] M. Buck, M. Karplus, Hydrogen bond energetics: A simulation and statistical analysis of N-methyl acetamide (NMA), water, and human lysozyme, Journal of Physical Chemistry B 105 (2001) 11000–11015.

[40] Z.-Z. Yang, P. Qian, A study of N-methylacetamide in water clusters: Based on atom-bond electronegativity equalization method fused into molecular mechanics, The Journal of Chemical Physics 125 (2006) 064311.

[41] W. L. Jorgensen, J. Gao, Cis-Trans energy difference for the peptide bond in the gas phase and in aqueous solution, J. Am. Chem. Soc. 110 (1988) 4212–4216.

[42] G. Nandini, D. N. Sathyanarayana, Ab initio studies on geometry and vibrational spectra of N-methylformamide and N-methylacetamide, J. Mol. Struct.(TEOCHEM) 579 (2002) 1–9.

[43] S. Shin, A. Kurawaki, Y. Hamada, K. Shinya, K. Ohno, A. Tohara, M. Sato, Conformational behavior of N-methylformamide in the gas, matrix, and solution states as revealed by IR and NMR spectroscopic measurements and by theoretical calculations, J. Mol. Struct. 791 (2006) 30–40.

[44] A. C. Fantoni, W. Caminati, Rotational spectrum and ab initio calculations of N-methylformamide, J. Chem. Soc., Faraday Trans. 92 (1996) 343–346.

[45] Y. K. Kang, H. S. Park, Internal rotation about the CN bond of amides, J. Mol. Struct.(TEOCHEM) 676 (2004) 171–176.

[46] H. Torii, T. Tatsumi, M. Tasumi, Effects of hydration on the structure, vibrational wavenumbers, vibrational force field and resonance raman

intensities ofN-methylacetamide, Journal of Raman Spectroscopy 29 (1998) 537–546.

[47] M. P. Gaigeot, Theoretical spectroscopy of floppy peptides at room temperature. A DFTMD perspective: Gas and aqueous phase, Physical Chemistry Chemical Physics 12 (2010) 3336–3359.

[48] F. Ingrosso, G. Monard, M. Hamdi Farag, A. Bastida, M. F. Ruiz-Lopez, Importance of Polarization and Charge Transfer Effects to Model the Infrared Spectra of Peptides in Solution, Journal of Chemical Theory and Computation 7 (2011) 1840–1849.

[49] K. Kwac, M. Cho, Molecular dynamics simulation study of N -methylacetamide in water. I. Amide I mode frequency fluctuation, The Journal of Chemical Physics 119 (2003) 2247–2255.

[50] S. Ham, J.-H. Kim, H. Lee, M. Cho, Correlation between electronic and molecular structure distortions and vibrational properties. II. Amide I modes of NMAnD2O complexes, The Journal of Chemical Physics 118 (2003) 3491–3498.

[51] M. Falk, T. A. Ford, Infrared spectrum and structure of liquid water, Can. J. Chem. 44 (1966) 1699–1707.

[52] D. F. Hornig, On the spectrum and structure of water and ionic solutions, J. Chem. Phys. 40 (1964) 3119.

[53] J. Stangret, Solute-affected vibrational spectra of water in $Ca(ClO_4)_2$ aqueous solution, Spect. Lett. 21 (1988) 369–381.

[54] J. Stangret, T. Gampe, Hydration sphere of tetrabutylammonium cation. FTIR of HDO spectra, J. Phys. Chem. B 103 (1988) 3778–3783.

[55] J. Stangret, T. Gampe, Ionic hydration behavior derived from infrared spectra in HDO, J. Phys. Chem. A 106 (2002) 5393–5402.

[56] M. Smiechowski, J. Stangret, Vibrational spectroscopy of semiheavy water (HDO) as a probe of solute hydration, Pure Appl. Chem. 82 (2010) 1869–1887.

[57] R. M. Badger, B. S. H. Bauer, Spectroscopic studies of the hydrogen bond II the shift of the OH vibrational frequency in the formation of the hydrogen bond, J. Chem. Phys. 5 (1937) 839–851.

[58] S. Bratos, J.-C. Leicknam, S. Pommeret, Relation between the OH stretching frequency and the OO distance in time-resolved infrared spectroscopy of hydrogen bonding, Chem. Phys. 359 (2009) 53–57.

[59] M. J. Frisch, G. W. Trucks, H. B. Schlegel, G. E. Scuseria, M. A. Robb, J. R. Cheeseman, G. Scalmani, V. Barone, B. Mennucci, G. A. Petersson, H. Nakatsuji, M. Caricato, X. Li, H. P. Hratchian, A. F. Izmaylov, J. Bloino, G. Zheng, J. L. Sonnenberg, M. Hada, M. Ehara, K. Toyota, R. Fukuda, J. Hasegawa, M. Ishida, T. Nakajima, Y. Honda, O. Kitao, H. Nakai, T. Vreven, J. A. Montgomery Jr., J. E. Peralta, F. Ogliaro, M. Bearpark, J. J. Heyd, E. Brothers, K. N. Kudin, V. N. Staroverov, R. Kobayashi, J. Normand, K. Raghavachari, A. Rendell, J. C. Burant, S. S. Iyengar, J. Tomasi, M. Cossi, N. Rega, J. M. Millam, M. Klene, J. E. Knox, J. B. Cross, V. Bakken, C. Adamo, J. Jaramillo,

R. Gomperts, R. E. Stratmann, O. Yazyev, A. J. Austin, R. Cammi, C. Pomelli, J. W. Ochterski, R. L. Martin, K. Morokuma, V. G. Zakrzewski, G. A. Voth, P. Salvador, J. J. Dannenberg, S. Dapprich, A. D. Daniels, Ö. Farkas, J. B. Foresman, J. V. Ortiz, J. Cioslowski, D. J. Fox, Gaussian 09, Revision D.01, 2009.

[60] E. R. Johnson, S. Keinan, P. Mori-Sanchez, J. Contreras-Garcia, A. J. Cohen, W. Yang, Revealing noncovalent interactions, Journal of the American Chemical Society 132 (2010) 6498–6506.

[61] T. Lu, F. Chen, Multiwfn: A multifunctional wavefunction analyzer, Journal of Computational Chemistry 33 (2012) 580–592.

[62] Taurine as a water structure breaker and protein stabilizer, Amino Acids 50 (2018) 125–140.

[63] C. Lee, W. Yang, R. G. Parr, Development of the colle-salvetti correlation-energy formula into a functional of the electron density, Physical Review B 37 (1988) 785–789.

[64] A. D. Becke, Density-functional thermochemistry. III. the role of exact exchange, The Journal of Chemical Physics 98 (1993) 5648–5652.

[65] R. Ditchfield, W. J. Hehre, J. A. Pople, Self-consistent molecular-orbital methods. IX. an extended gaussian-type basis for molecular-orbital studies of organic molecules, The Journal of Chemical Physics 54 (1971) 724–728.

[66] M. Cossi, N. Rega, G. Scalmani, V. Barone, Energies, structures, and

electronic properties of molecules in solution with the C-PCM solvation model, Journal of Computational Chemistry 24 (2003) 669–681.

[67] V. Barone, M. Cossi, Quantum calculation of molecular energies and energy gradients in solution by a conductor solvent model, Journal of Physical Chemistry A 102 (1998) 1995–2001.

[68] S. Grimme, S. Ehrlich, L. Goerigk, Effect of the damping function in dispersion corrected density functional theory, Journal of Computational Chemistry 32 (2011) 1456–1465.

[69] D. Eisenberg, W. Kauzmann, The Structure and Properties of Water., Oxford University Press, 1969.

Table 1: The parameters of HDO bands of water affected by NMA (Figure 1a), water affected by DMA (Figure 1b), "bulk" water (Figure 1c), and the respective intermolecular oxygen–oxygen distances. R_{OO} errors have been estimated on the basis of the HDO bands position errors.

T [a]	N [b]	$\nu^o{}_{OD}$ [c]	$\nu^g{}_{OD}$ [d]	$fwhh$ [e]	I [f]	$R^o{}_{OO}$ [g]	$R^g{}_{OO}$ [h]
NMA-affected water spectrum							
25	3.0±0.5	2505±2	2486±2	177±4	13120	2.821±0.003	2.821±0.003
35	2.8±0.5	2517±2	2492±2	178±4	11836	2.821±0.003	2.828±0.003
45	2.6±0.5	2518±2	2495±2	167±4	10640	2.836±0.003	2.833±0.003
55	2.5±0.5	2526±2	2501±2	175±4	10059	2.836±0.003	2.838±0.003
65	2.4±0.5	2526±2	2505±2	175±4	9400	2.841±0.003	2.844±0.003
75	2.2±0.5	2534±2	2511±2	169±4	8447	2.851±0.003	2.849±0.003
DMA-affected water spectrum							
25	2.5±0.5	2517±2	2497±2	165±4	16169	2.836±0.003	2.836±0.003
35	2.5±0.5	2524±2	2503±2	167±4	14666	2.836±0.003	2.836±0.003
45	2.6±0.5	2528±2	2505±2	167±4	13467	2.841±0.003	2.841±0.003
55	2.5±0.5	2534±2	2511±2	166±4	12066	2.851±0.003	2.849±0.003
"bulk" water spectrum							
25	-	2509±2	2505±2	162±4	10434	2.826±0.003	2.844±0.003
35	-	2513±2	2509±2	164±4	10022	2.836±0.003	2.849±0.003
45	-	2519±2	2513±2	164±4	9670	2.836±0.003	2.854±0.003
55	-	2522±2	2517±2	167±4	9281	2.838±0.003	2.859±0.003
65	-	2528±2	2521±2	170±4	8965	2.844±0.003	2.861±0.003
75	-	2532±2	2524±2	169±4	8612	2.849±0.003	2.867±0.003

[a] Temperature (°C). [b] Affected number, equal to the number of moles of water affected by one mole of solute. [c] Band position at maximum (cm^{-1}). [d] Band position at gravity center (cm^{-1}). [e] Full width at half-height (cm^{-1}). [f] Integrated intensity ($dm^3 \cdot mol^{-1} \cdot cm^{-1}$). [g] The most probable O$\cdots$O distance (Å). [h] Mean O$\cdots$O distance (Å).

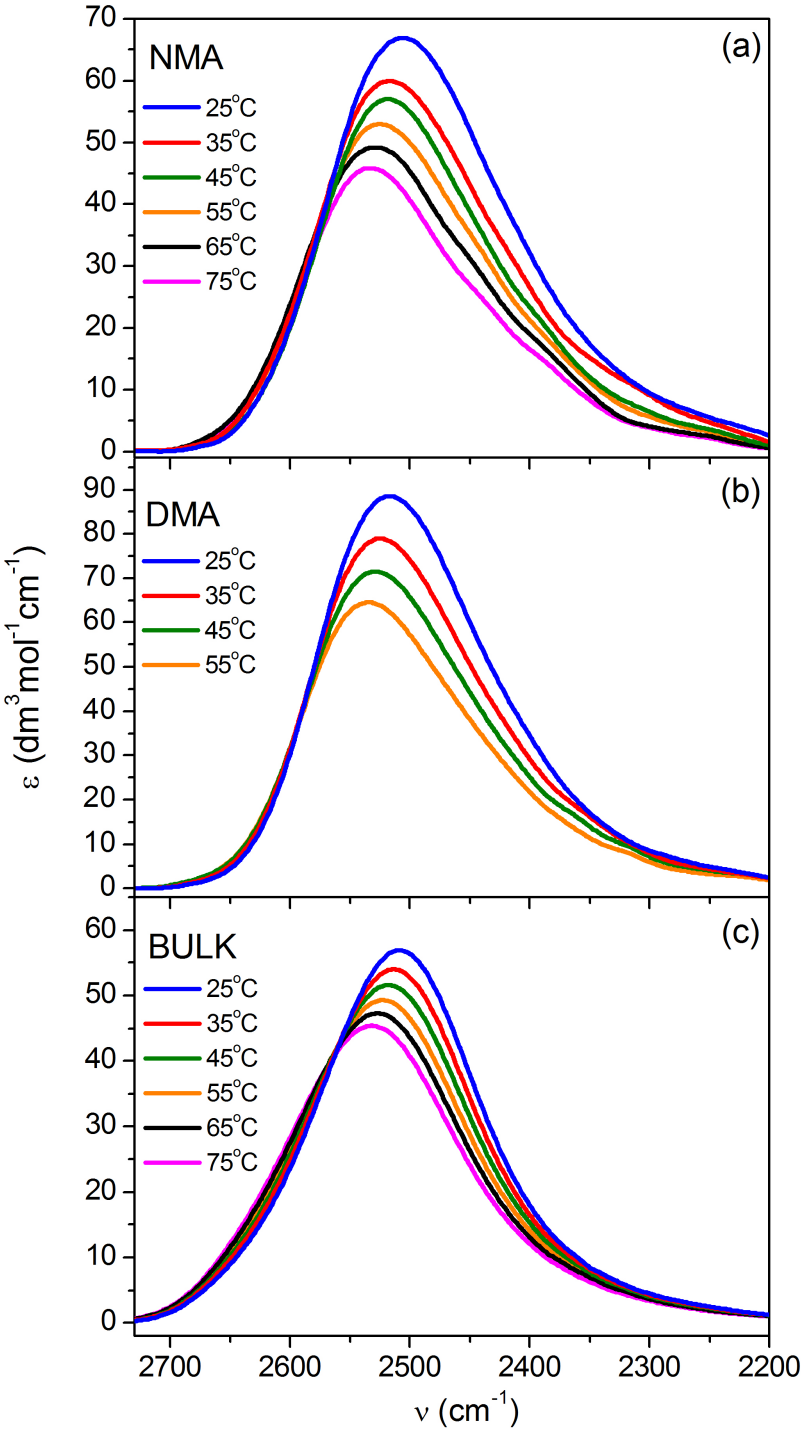

Figure 1: Solute-affected spectra in the OD stretching region for (a) NMA, (b) DMA, and (c) "bulk" HDO spectra as a function of temperature.

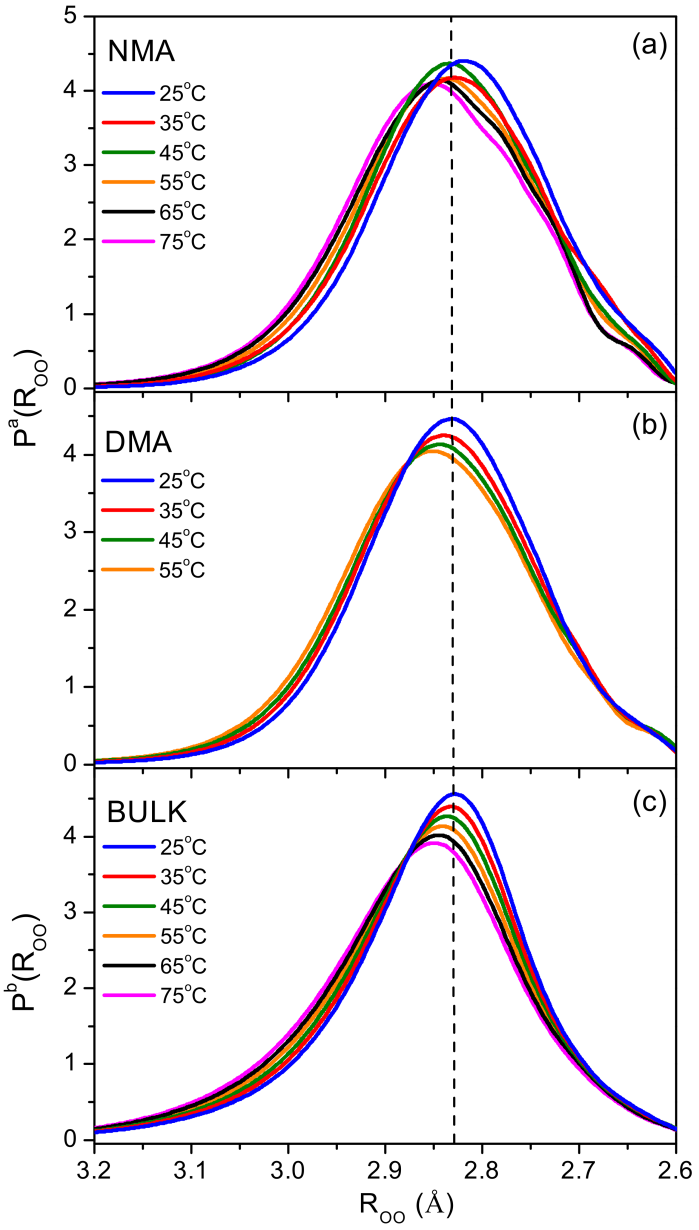

Figure 2: Interatomic oxygen-oxygen distance distributions function derived from the HDO spectra affected by (a) NMA, (b) DMA, and (c) "bulk" water spectra (Figure 1) for all studied temperatures. The vertical dashed line corresponds to the value of the most probable oxygen-oxygen distance in bulk water at 25 °C (2.826 Å, see Table 1).

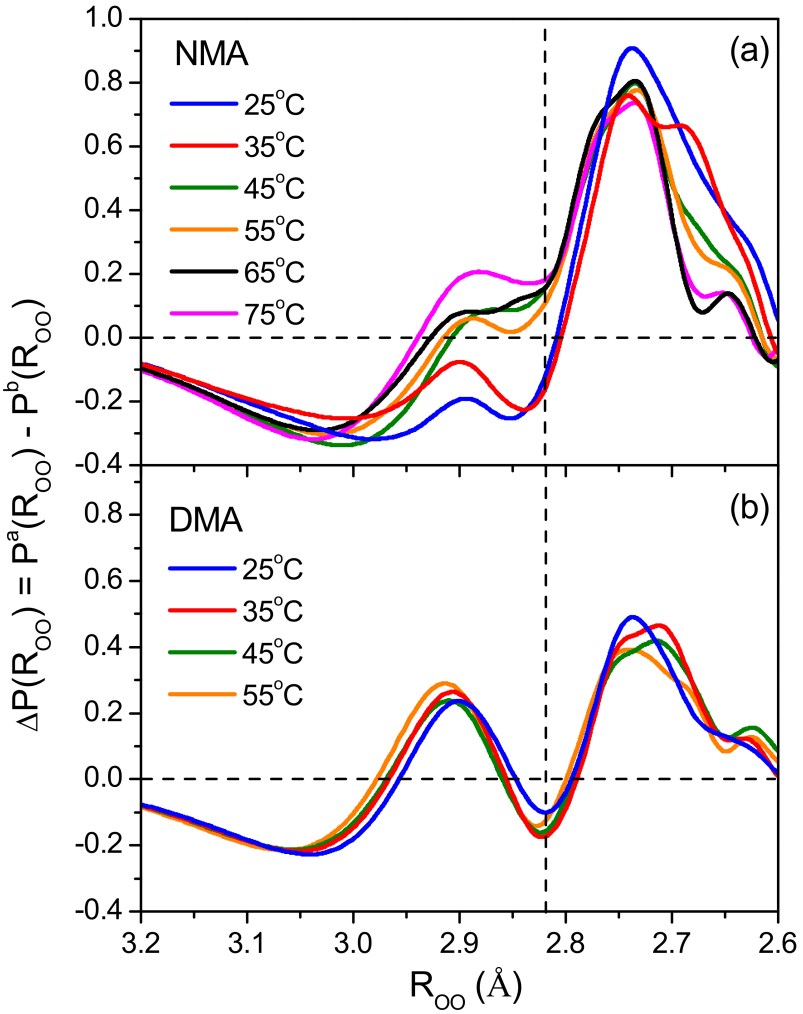

Figure 3: Differences between interatomic oxygen–oxygen distance distribution function of solute-affected water, $P^a(R_{OO})$, and the "bulk" water, $P^b(R_{OO})$, (Figure 2) at given temperature for (a) NMA and (b) DMA. The vertical dashed line corresponds to the value of the most probable oxygen-oxygen distance in bulk water at 25 °C (2.826 Å, see Table 1).

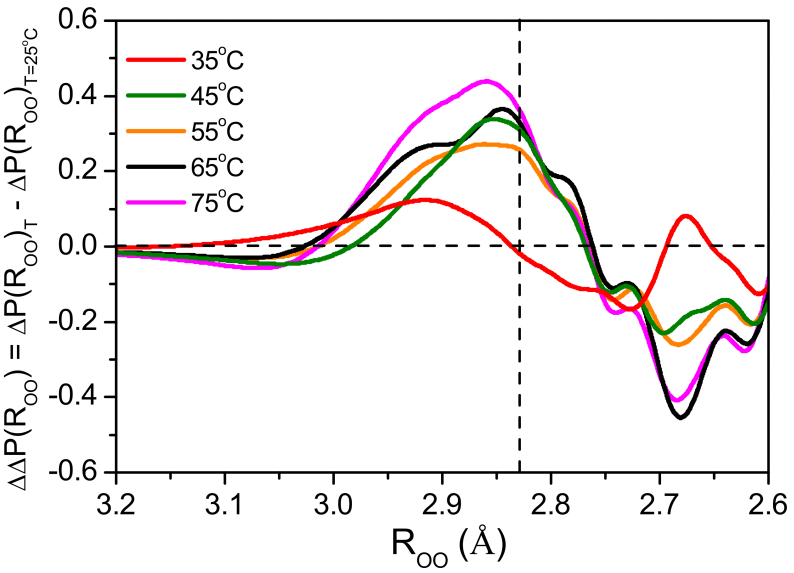

Figure 4: The result of subtraction of the oxygen-oxygen distance function at 25 °C, $\Delta P(R_{OO})_{25\,^{\circ}C}$, (blue line in Figure 3a) from the distance function at different temperatures, $\Delta P(R_{OO})_T$, obtained for NMA. The vertical dashed line shown to the position of the most probable oxygen-oxygen distance in bulk water at 25 °C (2.826 Å, see Table 1).

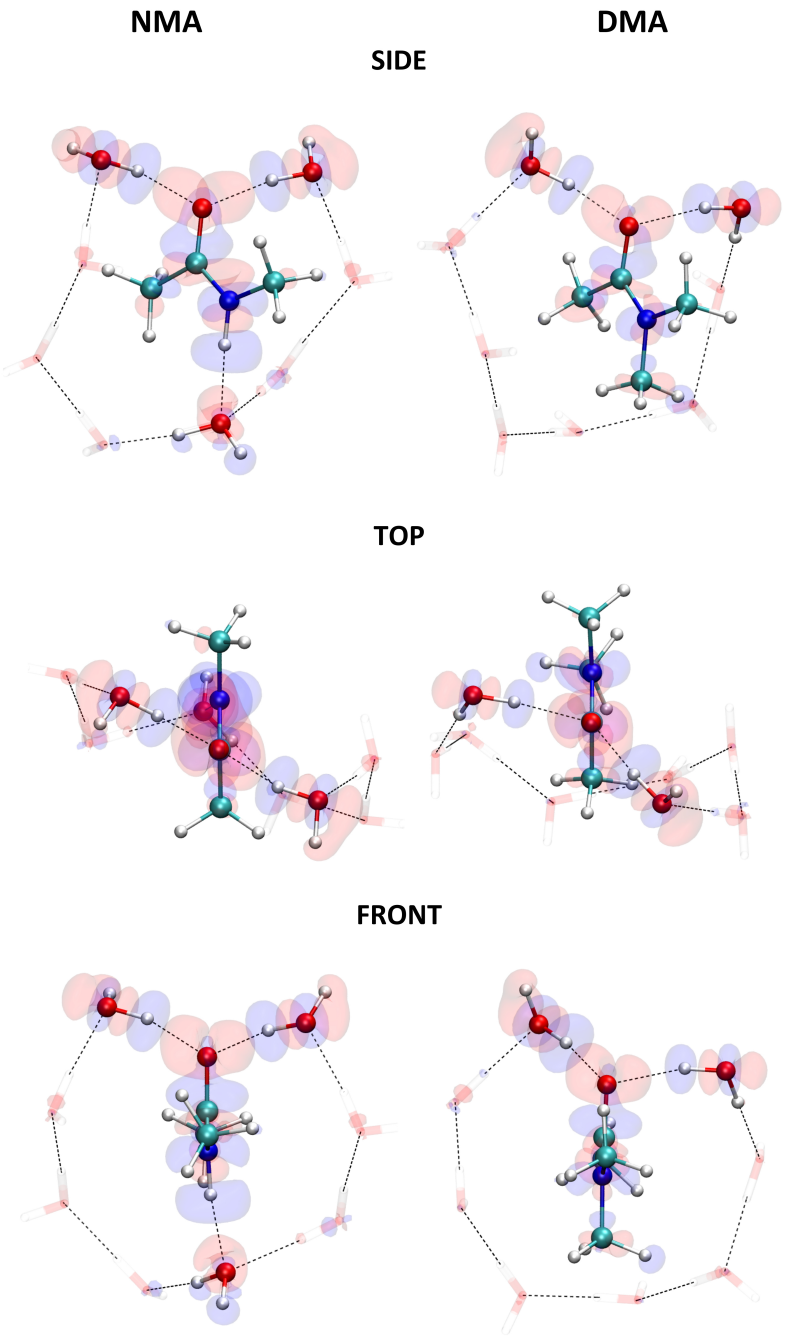

Figure 5: Differences in electron density of NMA and DMA complexes with water molecules caused by interactions of a central molecule with the water ring. Red regions correspond to increase of the electron density, blue regions mark its decrease. Additional movie files with the same structures are available in Supplementary Data.

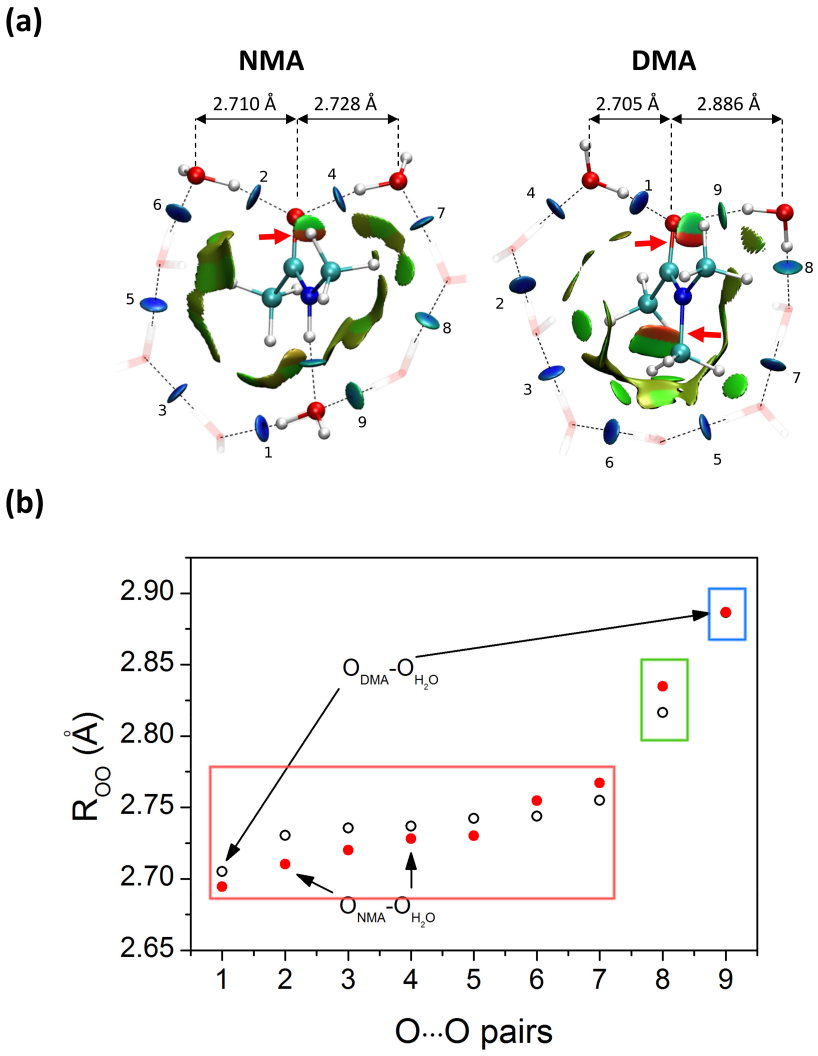

Figure 6: (a) Visualization of weak interactions in NMA and DMA complexes with water molecules. Blue disks correspond to hydrogen bonds, green/olive patches correspond to weak van der Waals interactions, red (marked with red arrows) correspond to steric repulsion. Selected water molecules are made transparent for clarity. Hydrogen bonds are marked with dashed black lines. Numbers indicate O···O pairs sorted according to their length (as in Figure b). Additional movie files with the same structures are available in Supplementary Data. (b) Distribution of oxygen···oxygen distances in NMA (red) and DMA (white) complexes with water. Only distances shorter than 3 Å are shown, and pairs corresponding to interaction of water molecules with the carbonyl oxygen are marked with arrows. The O···O pairs in red, green, or blue frames correspond to strengthened, "bulk-like", and weakened hydrogen bonds, respectively.